CREEP DEFORMATION AND RUPTURE OF OXIDE DISPERSION STRENGTHENED INCONEL MA 754 AND MA 6000E

T. E. Howson, F. Cosandey and J. K. Tien

Henry Krumb School of Mines, Columbia University
New York, NY 10027

Creep and stress rupture properties of the ODS mechanical alloys Inconel MA 754 and MA 6000E are presented. The properties are discussed with respect to those of more conventional alloys and dissected in terms of current threshold stress models for creep. The effects of HIP, notches and small prestrains, and cyclic creep and stress rupture results, showing both cyclic acceleration and deceleration, are also included.

INTRODUCTION

Advances in fabrication and thermomechanical treatments have given rise to new generations of oxide dispersion strengthened (ODS) alloys and superalloys for high temperature applications. Two of these ODS materials are INCONEL* alloys MA 754 and the experimental alloy MA 6000E, both made by the powder metallurgical process of mechanical alloying (1). In what follows the results of our ongoing study of the creep and stress rupture behavior of these mechanical alloys will be reviewed and discussed. Included in this investigation are the effects of prior small deformations, notches, hot isostatic pressure and cyclic loading.

EXPERIMENTAL RESULTS

The Alloys

MA 754 is an ODS nickel base solid solution, its com-

*Trademark of the INCO family of companies.

position by weight is nominally Ni-20%Cr-0.5%Ti-0.3%Al-0.05%C -0.6%Y_2O_3. The MA 754 used in this study also contained 1.3% Fe, 0.3% O and 0.13% N by weight. MA 6000E is a more highly alloyed ODS nickel-base superalloy strengthened by both oxide dispersoids and a high volume fraction of γ' precipitates. Its nominal composition by weight is Ni-15%Cr-4.5%Al-2.5%Ti-4%W-2%Ta-2%Mo-0.5%C-0.15%Zr-0.1%B-1.1%Y_2O_3. The γ' volume fraction in this alloy is about 50%. Both alloys are characterized by an elongated grain structure with a high grain aspect ratio (GAR) for high temperature strength. In the recrystallized state, MA 754 has a relatively fine grain size, with a longitudinal grain dimension of about 500 μm and a GAR of 5 to 10. The grain structure of the MA 6000E used in this study was much coarser, having transverse grain dimensions of about 1 mm and a GAR equal to or greater than 10.

The microstructure of MA 754, Fig. 1, consists of uniformly dispersed yttrium-aluminum oxides ranging in size from 10 to 100 nm and relatively large inclusions tentatively identified as titanium carbonitrides and yttria-aluminates, found at grain boundaries and in the matrix. A high twin density and a low dislocation density were also found randomly spaced in the matrix.

The microstructure of MA 6000E, Fig. 2, features a unique duplex structure of dispersoids and precipitates. Oxide particles ranging in size from 10 to 100 nm are dispersed throughout both the matrix phase and the uniformly spaced 0.2 μm diameter γ' particles that make up about 50 volume percent. MA 6000E has fewer inclusions and a lower density of twins than MA 754.

Creep Behavior

Specimens for tensile creep testing in air under constant load were cut parallel to the longitudinal grain direction. Creep results for MA 754 (2) and MA 6000E (3) are shown in the double logarithmic plots of steady state creep rates $\dot{\varepsilon}_s$ versus applied stresses σ, Figs. 3 and 4. For both alloys, a power law relation is obeyed over the stress ranges studied and, as is characteristic of many alloys strengthened by a second phase, the stress dependence of the secondary creep rate is high. The values of the stress exponent $n = [\delta \ln \dot{\varepsilon}_s / \delta \ln \sigma]_T$ range from 19 to 50. The apparent creep activation energies for these alloys determined between 746° and 774°C from plots of $\ln \dot{\varepsilon}_s$ versus 1/T were found to be 2 to 3 times

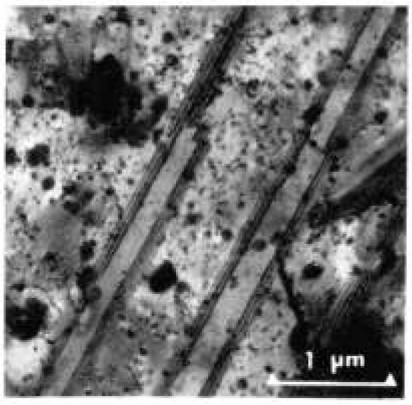

Fig. 1. Bright field TEM micrograph showing the microstructure of MA 754.

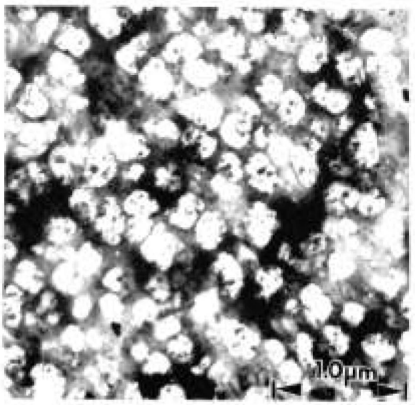

Fig. 2. Dark field TEM micrograph showing the γ' precipitates and the dispersoids in MA 6000E.

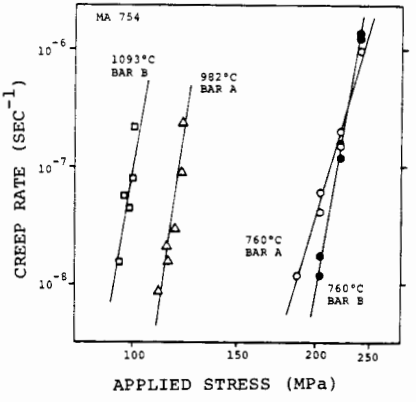

Fig. 3. Stress dependence of the minimum creep rate in MA 754 at 760°, 982°, and 1093°C.

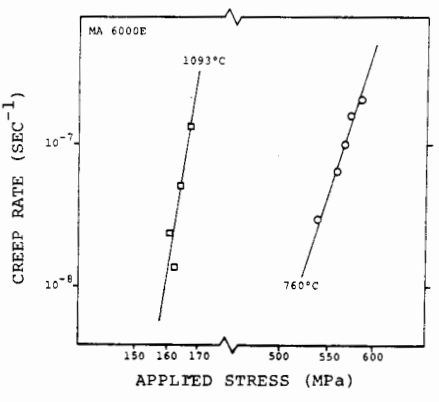

Fig. 4. Stress dependence of the minimum creep rates in MA 6000E at 760° and 1093°C.

greater than the activation energy for self diffusion of nickel. By taking into account the temperature dependence of the modulus (4), which introduces a correction term to the apparent creep activation energy, a creep activation energy close to but slightly greater than the nickel self diffusion energy was obtained for MA 754. For MA 6000E, the creep activation energy remained twice the self diffusion energy even after the modulus correction.

Examination of crept MA 754 in the transmission electron microscope (TEM) showed dislocations pinned at and bowing between the oxide dispersoids over the whole range of stresses and temperatures studied. A typical micrograph is shown in Fig. 5. No dislocation substructure formation was observed in MA 754 or in MA 6000E. In MA 6000E crept at 760°C, Fig. 6, stacking faults, evidence of dislocation shearing of γ' are seen. This feature is not seen after 1093°C creep.

Stress Rupture Behavior

Log-log plots of applied stress versus stress rupture life are shown in Figs. 7 and 8. The shallow slopes of these plots emphasize the sensitivity of the creep deformation to the applied stress level as reflected by the high stress exponents. Fig. 7 includes stress rupture data obtained with transverse specimens of MA 754 and shows that the 100-hour transverse rupture strength of MA 754 is less than the 100-hour longitudinal rupture strength by about 27% and 59% at 760°and 982°C, respectively. The transverse strength of MA 6000E could not be tested due to the non-availability of large diameter bars. The stress rupture strengths of MA 754 and MA 6000E are compared to the stress rupture strengths of other nickel-base ODS alloys and superalloys in Fig. 9. in which the stresses for rupture in 100 hours are plotted as a function of temperature. At intermediate temperatures, MA 6000E has stress rupture strength that is equal to that attained in most conventional nickel-base superalloys, while at elevated temperatures the stress rupture strength of MA 6000E is superior to all other ODS materials. MA 754 also has excellent stress rupture strength at elevated temperatures.

Stress rupture in fine grained MA 754 was intergranular at all strain rates and temperatures studied and appeared to occur as a result of cavitation and cracking at transverse grain boundaries. A typical optical photomicrograph of cavitation and cracking at transverse grain boundaries is shown in Fig. 10. Many intergranular voids in MA 754 are associated

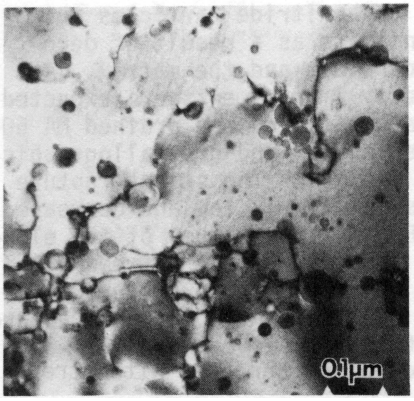

Fig. 5. A typical TEM micrograph of MA 754 crept at 760°C and 220 MPa showing dislocation pinning at dispersoids.

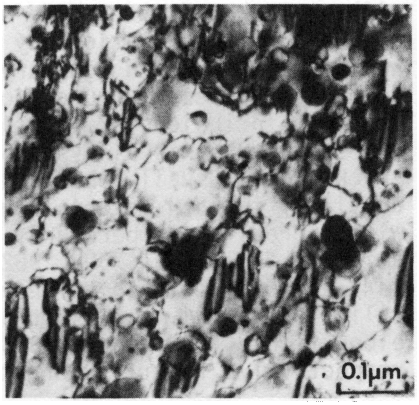

Fig. 6. A TEM micrograph of MA 6000E crept at 760°C and 586 MPa, showing stacking fault fringes indicative of dislocation shearing of γ' and dislocation pinning at dispersoids.

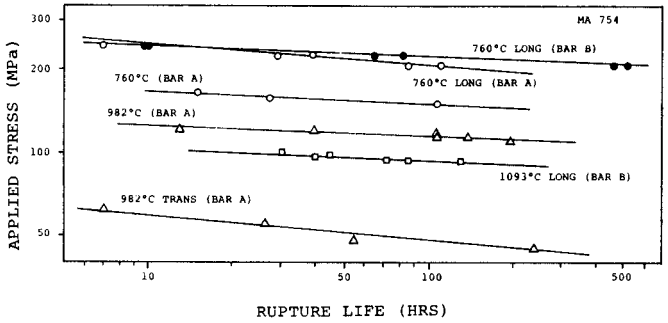

Fig. 7. Rupture lives as a function of applied stresses in MA 754 for specimens oriented parallel (LONG) and perpendicular (TRANS) to the extrusion axis.

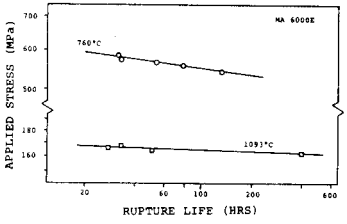

Fig. 8. Rupture life versus applied stress for MA 6000E at 760° and 1093°C.

with grain boundary carbide or carbonitride particles which suggests that cavitation may initiate as a result of decohesion between grain boundary carbides and the matrix. Accordingly, stress rupture property improvements are expected when the inclusions are eliminated. In coarse grained MA 6000E stress rupture was always transgranular and crystallographic cracking was usually observed, Fig. 11. The stress rupture ductility in both materials was relatively low and decreased with increasing temperature. For MA 754, values of the elongation to failure of 760°, 982° and 1093°C fell between 4-16%, 1-4% and 0.5-2%, respectively. The transverse rupture ductility in MA 754 was less than 4%. For MA 6000E, the rupture elongation at 760° and 1093°C fell between 2-6% and 0.5-3%, respectively. Rupture elongation also increased with stress.

Notch, HIP, Predeformation and Cyclic Loading Effects

Additional studies have been carried out with MA 754 to determine any possible effects of notches (5) and small predeformations (6,7) on the creep and stress rupture behavior. The introduction of notches into longitudinal specimens increased the rupture life in MA 754 by factors up to 16 at 760°C, Fig. 12. This may be the first reporting of stress rupture notch strengthening in an alloy with limited ductility. Notch strengthening was observed in specimens with elastic stress concentration factors of 3 and 10, and this notch strengthening increased with stress.

Several different hot isostatic pressing (HIP) treatments were used to effect small localized deformations in MA 754 before creep and stress rupture testing (6). Although the HIP process is a hydrostatic compression, localized plastic flow occurred at regions of incompatibility such as grain boundaries or large inclusions, Fig. 13, due to the existence of deviatoric components of stress in these regions. Creep and stress rupture testing of HIP-treated material was carried out at 760° and 1093°C. The HIP exposures generally resulted in small but consistent improvements in the subsequent 760°C creep and stress rupture resistance, see for example Fig. 14, but the HIP treatments did not appear to affect the 1093°C creep and stress rupture behavior of MA 754. Stress rupture ductilities were not affected by the HIP exposures.

Another predeformation was obtained by carrying out small amounts of high strain rate creep deformation at 760°C (7). The prestrains were kept small to ensure that no cracks were introduced into the material. Precracking would only cause

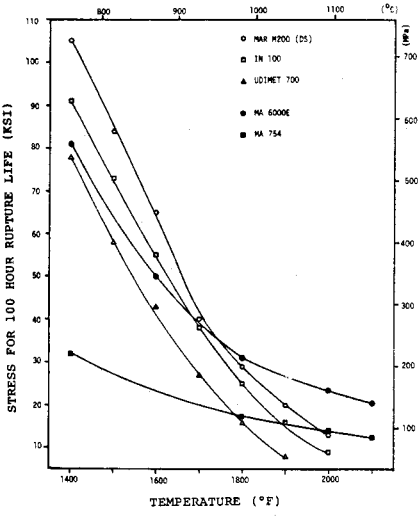

Fig. 9. The stresses to cause creep rupture at 100 hours as a function of temperature for MA 6000E, MA 754 and several nickel-base superalloys.

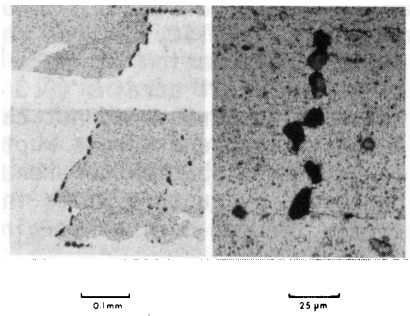

Fig. 10. Photomicrographs of MA 754 showing void formation and cracking after creep at 760°C and 207 MPa.

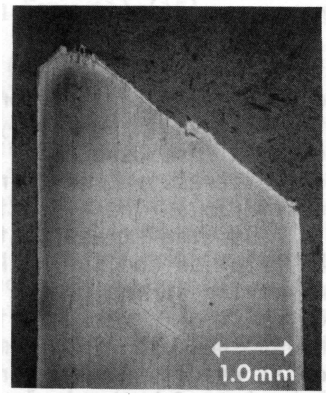

Fig. 11. Photomicrograph of a failed specimen of MA 6000E crept at 1093°C and 160 MPa.

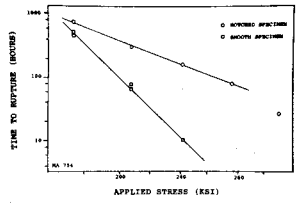

Fig. 12. Rupture lives as a function of applied stress for smooth and notched (K_t = 3) specimens of MA 754 at 760°C.

a degradation of the creep and stress rupture resistance. Specimens were subsequently crept to failure at the same temperature under a lower stress. As with the HIP exposure, this pretreatment caused localized plastic deformation at regions of incompatibility such as inclusions and grain boundaries, but the deformation was more homogeneous than that caused by HIP. The small strains (0.3 to 1.2%) accumulated at 760°C with a high stress did not cause any degradation in the subsequent creep and stress rupture properties at 760°C and a lower stress, but rather resulted in small improvements, as reflected by rupture lives increased up to 25% and significantly reduced minimum strain rates, Fig. 15.

Preliminary results on the cyclic creep behavior of MA 754 at 760°C are shown in Fig. 16 for load cycling between 220.7 MPa and 41.4 MPa and cycle periods of 10 hrs, 2 hrs, 20 min and 10 min. For the longer loading time of 5 hrs, cyclic weakening is observed -- the total time at load during the cyclic creep test is less than the time to rupture for the creep test in which the load is not cycled. As the loading time is decreased, a transition to cyclic strengthening occurs. For the loading times of 10 min and especially 5 min, the total time at load during the cyclic creep test is greater than the time to rupture for the creep test in which the load is not cycled.

DISCUSSION

The creep behavior of many metals and alloys, and in particular, the unusual high stress dependence and activation energy of creep deformation in particle strengthened alloys has been rationalized by describing the stress dependence of the creep rate in terms of an effective stress rather than simply in terms of the applied stress (8-15). The effective stress is the applied stress minus a resisting stress that represents a threshold stress or the friction and the back stresses experienced by dislocations moving during creep. Several investigators have measured resisting stresses using stress change experiments, and although there is disagreement over the interpretation of experimental results (and a confusion in terminology), the creep behavior of both simple and complex materials has been successfully described with the effective stress concept.

The creep behaviors of MA 754 and MA 6000E were also analyzed by formulating a description of creep that incorporated a resisting stress. In this work, a curve fitting

procedure was used to identify the resisting stresses due to the second phase particles in MA 754 and MA 6000E (2,3,14,15). These values were found to compare well with calculated values of the stresses required for the process of mobile dislocation bypass of the strengthening particles, at the creep test temperatures and creep strain rates. Carried further the analysis was able to identify other contributions to the resisting stress including the component due to solute strengthening of the matrix phase (15). This approach resulted in a generalized creep expression,

$$\dot{\varepsilon}_s = A(1-k)^{no}[(\sigma_a-\sigma_p)/E]^{no}\exp(-Q/RT) \qquad (1)$$

in which $\dot{\varepsilon}_s$ is the steady-state creep rate, A is a structure and material dependent constant, k is a constant between 0 and 1 that represents the amount of solid solution strengthening in the matrix, σ_a is the applied stress, σ_p is the resisting stress due to the strengthening second phase particles, E is the Young's modulus, Q is the creep activation energy, R is the gas constant and T is the temperature. Values of the resisting stress terms have been determined for MA 754 and MA 6000E from experimental data at 760°C (15). The creep behavior of a wide range of particle strengthened alloys including both ODS alloys and superalloys has been rationalized using Eqn. (1) (15).

As mentioned, we found that pretreatment of MA 754 with HIP exposure or prior creep deformation causes inhomogeneous local plastic flow or dislocation generation at inclusions, dispersoids and grain boundaries. This increased dislocation density can account for the small improvements in the creep and stress rupture resistance of MA 754 after prior deformation. It is also possible that these predeformations serve to relieve any residual stresses at grain boundaries and second phase particles. Such a process might effectively inhibit the decohesion that marks the onset of stress rupture in MA 754 and thereby enhance the stress rupture resistance of this alloy.

Similarly, it is possible that the notch strengthening observed for MA 754 is due to the initial localized plastic flow that occurs at the root of the notch which, through dislocation generation or relaxation of residual stresses, enhances the creep and stress rupture resistance of the material. The notch strengthening effect may also be explained by geometrical considerations. The very short gage length of a

notched specimen contains few transverse grain boundaries due to the elongated grain structure in MA 754. The notch test, then, may represent a test of the strength of the dispersion strengthened matrix rather than a test of the strength of the matrix plus grain boundaries.

Our initial cyclic creep and stress rupture results for MA 754 are interesting, not only because these are the first reported data on the creep and stress rupture behavior during cyclic loading of an ODS alloy but also because both cyclic strengthening and cyclic weakening were observed. This finding has ramifications with respect to the basic understanding of cyclic creep and stress rupture in general.

ACKNOWLEDGEMENT

We are grateful to AFOSR for supporting this work under grant AFOSR-78-3637A, and to NASA-Lewis for supplying material for study.

REFERENCES

1. J.S. Benjamin, Met. Trans. 1, 2943 (1970).
2. T.E. Howson, J.E. Stulga and J.K. Tien, "Creep and Stress Rupture of Oxide Dispersion Strengthened Mechanically Alloyed Inconel Alloy MA 754," accepted for publication in Met. Trans. A, 1980.
3. T.E. Howson, D.A. Mervyn and J.K. Tien, "Creep and Stress Rupture of a Mechanically Alloyed Oxide Dispersion and Precipitation Strengthened Nickel-Base Superalloy," accepted for publication in Met. Trans. A, 1980.
4. M. Malu and J.K. Tien, Scripta Met. 9, 1117 (1975).
5. F. Nami, M.S. Thesis, Columbia University, New York (1979).
6. A. Koren, M.S. Thesis, Columbia University, New York (1979).
7. R.T. Marlin, F. Cosandey and J.K. Tien, "The Effect of Predeformation on the Creep and Stress Rupture of an Oxide Dispersion Strengthened Mechanical Alloy," submitted to Met. Trans. A, 1980.
8. A.A. Soloman and W.D. Nix, Acta Met. 18, 863 (1970).
9. M. Pahutová and J. Cadek, Mater. Sci. Eng. 11, 151 (1973).
10. P.W. Davies, G. Nelmes, K.R. Williams and B. Wilshire, Met. Sci. J. 7, 87 (1973).
11. R. Lagneborg and B. Bergman, Met. Sci. 10, 20 (1976).
12. W.J. Evans and G.F. Harrison, Met. Sci. 10, 307 (1976).
13. R.W. Lund and W.D. Nix, Acta Met. 24, 469 (1976).

14. S. Purushothaman and J.K. Tien, Acta Met. 26, 519 (1978).
15. O. Ajaja, T.E. Howson, S. Purushothaman and J.K. Tien, "Role of Alloy Matrix in the Creep Behavior of Particle Strengthened Alloys," accepted for publication in Mater. Sci. Eng., 1980.

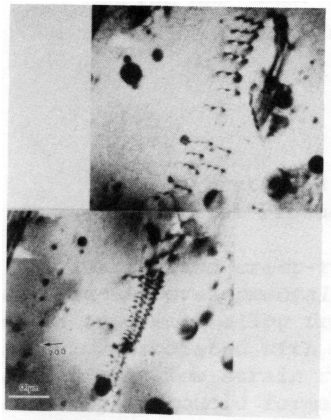

Fig. 13. Dislocation emission in MA 754 from a particle-matrix interface due to HIP exposure of 1177°C/138 MPa/ 2 hrs.

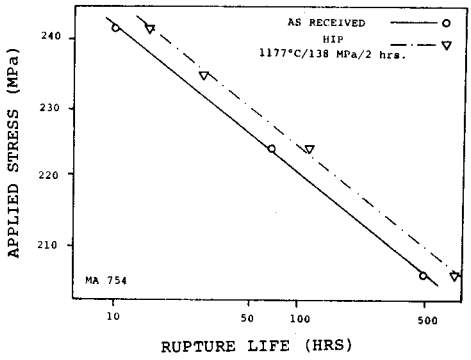

Fig. 14. Dependence of rupture life on applied stress in MA 754 for as-received material and for material after HIP exposure.

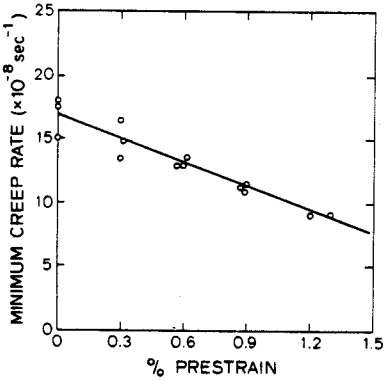

Fig. 15. Minimum 760°C creep rate as a function of 760°C tensile creep prestrain.

CYCLIC PERIOD*	RUPTURE LIFE (TIME ON MAX. LOAD)	RATIO CYCLIC RUPTURE TIME (ON UPPER LOAD) / STATIC RUPTURE LIFE
10 HR	47 HR	0.85
2 HR	55.5 HR	1.01
0.33 HR	58 HR	1.05
0.17 HR	180 HR	3.27
(STATIC @ 220 MPa)	(55 HR)	

Fig. 16. Preliminary cyclic creep results at 760°C for MA 754.